

Spin-Orbit Relaxation Rates of Bi($6p^3, ^2D_{3/2}$) following Photolysis of Bi(CH₃)₃ at $\lambda = 193$ nm

J. S. Holloway,* J. B. Koffend, and R. F. Heidner III

Aerophysics Laboratory, The Aerospace Corporation, P.O. Box 92957, Los Angeles, California 90009
(Received: March 29, 1989; In Final Form: May 30, 1989)

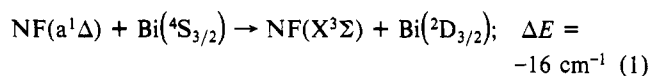
Rate coefficients for the collisional relaxation of the first excited spin-orbit state of Bi ($6p^3, ^2D_{3/2}$) have been measured at 295 K for Ar, CO₂, SF₆, H₂, D₂, HF, and DF. The excited Bi atoms were prepared by excimer laser photolysis of trimethylbismuth (TMB) at 193 nm and monitored directly in emission. The rate coefficient for quenching by the precursor TMB and a lower limit for removal by CH₃ photofragments have also been established. Where applicable, our results are compared with the earlier work of Bevan and Husain and of Trainor. The suitability of long-range interaction models is discussed for those cases where isotopic substitution leads to markedly different quenching rates.

I. Introduction

The collisional behavior of the first two excited spin-orbit states of the bismuth $6p^3$ ground-state configuration ($^2D_{3/2,5/2}$) has been the subject of a number of investigations.¹⁻⁴ Because they share the same electronic configuration as the $^4S_{3/2}$ ground state, these states are optically metastable. As such they provide a convenient venue for the study of collisional relaxation of electronically excited atoms. In turn, the results of these experiments have been useful in understanding heavy atom-molecule collisions and the strengths and limitations of employing (J, Ω) coupling approximations in treating them. Quenching studies of low-lying spin-orbit states have also provided direct evidence of electronic-to-vibrational ($E \rightarrow V$) energy transfer.⁵

The development of electronic transition lasers has also required an increased understanding of the kinetics of metastable atoms. As an example, the 472-nm pulsed Bi vapor laser terminates on the $^2D_{3/2}$ level.⁶ Knowledge of that state's relaxation and removal processes is critical to evaluation of the device's performance.

Our laboratory's interest in low-lying Bi metastables dates from the discovery of the efficient, near-resonant electronic energy transfer between the first excited state of nitrogen fluoride and the ground state of Bi:⁷



Reanalysis of this experiment, in light of the subsequently reported lifetime of NF($a^1\Delta$) of 5.6 s,⁸ gives a rate constant, $k_1 = 1.8 \times 10^{-10} \text{ cm}^3/(\text{molecule}\cdot\text{s})$. It has been postulated that Bi($^2D_{3/2}$) can further react with another NF($a^1\Delta$) molecule to produce electronically excited BiF:⁹



Evidence suggests that this reaction is both fast (ca. $8 \times 10^{-11} \text{ cm}^3/(\text{molecule}\cdot\text{s})$) and selective, creating the potential for a

population inversion on the BiF($\text{AO}^+ \rightarrow \text{XO}^+$) transition in the 430-480-nm spectral region. Employing densities of NF($a^1\Delta$) on the order of 10^{10} cm^{-3} , virtually complete inversions of Bi($^2D_{3/2}$) have been achieved at the 10^8 cm^{-3} number density level.¹⁰ In experiments scaled to higher densities ($[\text{NF}(a^1\Delta)] \approx 10^{13} \text{ cm}^{-3}$, $[\text{Bi}] \approx 10^{10} \text{ cm}^{-3}$), it was found that a substantial fraction of the available Bi was converted to BiF, with strong emission observed from the blue BiF(A \rightarrow X) band system.¹¹

NF($a^1\Delta$) is conveniently produced by means of the H₂/NF₂ chain reaction¹²



in which reaction 4 produces the $a^1\Delta$ state with a branching ratio of >0.9 .^{8,13} Thus, we have a system capable of producing a reservoir of chemical energy in extremely high yield (reactions 3 and 4) which may be coupled to an efficient mechanism (reactions 1 and 2) for extracting that energy in the form of an electronically excited diatomic molecule with a radiative transition in the blue region of the visible spectrum. The system described is a promising visible chemical laser candidate.¹⁴

The purpose of the present study is to investigate those removal processes of Bi($^2D_{3/2}$) that pertain to the chemical milieu of the laser system. The current investigation has been limited to those cases in which nonreactive collisions are expected to be the dominant removal mechanism. The species of interest include H₂ (D₂) and HF (DF). A frequently employed photolytic source of Bi is trimethylbismuth (Bi(CH₃)₃; TMB); its rate coefficient also has been determined, as well as a lower limit for quenching by daughter CH₃ fragments. Additionally, rate coefficients for the inert gases Ar, SF₆, and CO₂ have been obtained.

II. Experimental Apparatus and Procedure

In approaching this study, we have tried not only to extend the available body of knowledge on the subject but also to improve upon the methodology of previous work. Earlier kinetics studies have relied on flash photolysis of TMB to generate the excited Bi atom population²⁻⁴ and resonant atomic absorption to monitor the 2D states. The broad-band ultraviolet output of the flash lamps was found to lead to the formation of a remarkably large number

(1) Connor, J.; Young, P. J.; Strausz, O. P. *J. Am. Chem. Soc.* **1971**, *93*, 822.

(2) Bevan, M. J.; Husain, D. *J. Phys. Chem.* **1976**, *80*, 217.

(3) Trainor, D. W. *J. Chem. Phys.* **1977**, *60*, 3094.

(4) Trainor, D. W. *J. Chem. Phys.* **1977**, *67*, 1206.

(5) Leone, S. R.; Wodarczyk, F. J. *J. Chem. Phys.* **1974**, *60*, 314.

(6) Deutsch, T. F.; Ehrlich, D. J.; Osgood, Jr., R. M. *Opt. Lett.* **1979**, *4*, 378.

(7) Capelle, G. A.; Sutton, D. G.; Steinfeld, J. I. *J. Chem. Phys.* **1978**, *69*, 5140.

(8) Malins, R. J.; Setser, D. W. *J. Phys. Chem.* **1981**, *85*, 1342.

(9) Herbelin, J. M. Efficient Production of Electronically Excited BiF(AO^+) via Collisions with NF(a). II. In *Proceedings of the International Conference on Lasers, 1986*; STS Press: McLean, VA, 1987; pp 281-288.

(10) Herbelin, J. M.; Klingberg, R. A. Short-Wavelength Chemical Lasers Based on the Nitrogen Fluoride Molecule; Aerospace Report No. ATR-82-(8498)-1, 1 Dec 1982, pp 67-70.

(11) Herbelin, J. M.; Klingberg, R. A. *Int. J. Chem. Kinet.* **1984**, *16*, 849.

(12) Koffend, J. B.; Heidner III, R. F.; Gardner, C. E. *J. Chem. Phys.* **1981**, *80*, 1861, and references therein.

(13) Heidner III, R. F.; Helvajian, H.; Holloway, J. S.; Koffend, J. B. To be published.

(14) Sutton, D. G.; Suchard, S. N. *Appl. Opt.* **1975**, *14*, 1898.

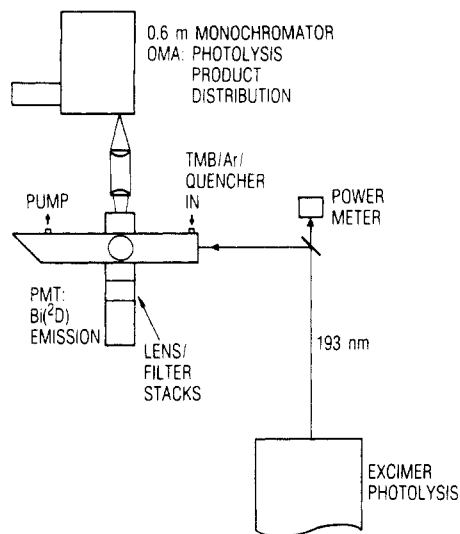


Figure 1. Block diagram of experimental arrangement.

of species,¹ while the relatively long duration of the pulse imposed a substantial lower limit on the temporal resolution of the experiments. Because the atomic states were monitored in absorption, the signal-to-noise ratio of those studies was determined by the characteristics of the line sources used.^{2,3} An additional complication encountered in the use of an absorption probe is the necessity of determining the experimental parameter γ in the modified Beer-Lambert expression¹⁵

$$I = I_0 \exp(-\epsilon(c)l\gamma)$$

where the symbols have their usual meaning. We have departed from past work in two significant respects. We have chosen ArF excimer laser photolysis of TMB at 193 nm to create our initial $\text{Bi}(^2\text{D}_{3/2})$ population. By so doing, we are able to deposit the photolysis energy into the parent species in a relatively well characterized manner. This approach also makes it much easier to discriminate against scattered light in our optical detection channel, thereby affording the experiment a time resolution limited in principle only by the 14-ns excimer pulse. Secondly, we observe $\text{Bi}(^2\text{D}_{3/2})$ directly in emission at 876 nm via a narrow-band interference filter and a red-sensitive GaAs photomultiplier tube. As a result, we have extremely sensitive detection and simplified data analysis by comparison to earlier work.

Our experimental layout is depicted schematically in Figure 1. It consists of a temperature-controlled flow reactor and associated gas-handling manifold, an excimer photolysis laser, and signal detection and acquisition instrumentation. The flow cell is of stainless steel construction, 25 cm in length by 4.6 cm i.d., internally coated with Teflon in order to reduce the rate of radical recombination at the walls. Three viewing ports are located at right angles to the flow axis, which is also the photolysis axis. Aluminum extension pieces, 15 cm in length, have been added to both ends of the cell. These allow for the addition of a purge on the entrance window and a stack of light baffles and a Brewster angle mount on the exit window. The purge is necessary to prevent the transmission of the window from degrading due to the accumulation of bismuth metal after a number of photolysis pulses. The baffles and Brewster window are used to reduce scattered excimer light. Suprasil windows are used on all cell ports for most of the experiments. These were replaced with CaF_2 windows on the observation ports and MgF_2 windows on the excimer photolysis ports for the quenching measurements with HF and DF.

Reagent gases were premixed and introduced in the central stainless steel/Teflon section of the cell. Flow rates were measured with mass flow meters (Tylan) which had been calibrated in situ. Pressure was measured by a capacitance manometer (MKS) with 10-mTorr resolution. Total flow rates were typically less than

1.0 L-atm/min. Overall cell pressure (on the order of 30–80 Torr) and the partial pressure of TMB (about 1×10^{-4} Torr for most runs) were held constant with Ar as the buffer gas for each set of measurements so that system heat capacity, diffusion, and $\text{Bi}(^2\text{D}_{3/2})$ removal by Ar and TMB would in turn be constant factors in each determination.

An excimer laser (Lambda Physik EMG 101) was operated with ArF at 193 nm to produce the 14-ns photolysis pulse. Because of the marked power dependence of the $\text{Bi}(^2\text{D}_{3/2})$ decay rate, we chose to attenuate the excimer output by means of a stack of fused silica flats to a level that resulted in reasonably long base-line decay times without sacrificing signal to noise. Photolysis fluences on the order of 5–10 mJ/cm² were typically used, although fluences as high as 60 mJ/cm² were employed for power dependence measurements. Energy was determined with a cavity type joulemeter (Laser Precision) to sample the fraction of 193-nm radiation transmitted by the excimer turning mirror and calibrated against a thermal power meter (Coherent) positioned directly in front of the entrance window of the cell. The experiments were conducted at repetition rates of 2.0–0.5 Hz to assure the removal of photolysis products between pulses.

Our diagnostics consist of a thermoelectrically cooled GaAs phototube (RCA C310134) which collects $\text{Bi}(^2\text{D}_{3/2})$ emission through a narrow-band interference filter (876.0 nm, 0.64 nm fwhm) following the photolysis of TMB. The signal is amplified (Tektronix 502) and collected with a transient digitizer (LeCroy 2264) and averaged with a laboratory computer (DEC LSI 11/73). Total photolysis emission is resolved with a 0.6-m monochromator (McPherson 207) and recorded with an optical multichannel analyzer (OMA; EG&G PARC 1461 with 1420BR intensified diode array).

A 0.1% mixture of trimethylbismuth (TMB) (ICN Pharmaceuticals) in Ar was used. Hydrogen fluoride and deuterium fluoride samples (Matheson) were purified by several freeze-pump-thaw cycles in a stainless steel vessel. The HF and DF were run as 20% mixtures diluted with Ar. The other reagents were as follows: Ar (Matheson UHP, 99.999%), CO₂ (Alphagaz Research Grade, 99.998%), H₂ (Matheson UHP, 99.999%), D₂ (98%), SF₆ (Matheson Instrument Purity, 99.99%).

III. Results and Discussion

We observe (in emission) a wide disposition in the energy of the Bi resulting from ArF laser photolysis of TMB. In OMA traces from 2200 to 6500 Å we can unambiguously identify 16 lines,¹⁶ which originate from 11 excited states of Bi with energies of up to almost 50 000 cm⁻¹. We also observe a blue-degraded band structure at about 4315 Å, which is probably attributable to Bi₂.

Of the 11 excited states lying above $\text{Bi}(^2\text{D}_{3/2})$ that we observe, all but the three other excited spin-orbit states of the 6p³ ground-state configuration ($^2\text{P}_{3/2,1/2}$ and $^2\text{D}_{5/2}$) possess dipole-allowed transitions to either $^4\text{S}^{\circ}$ or $^2\text{D}_{3/2}$. These states can reasonably be expected to be short-lived. Of the other 6p³ states, only $^2\text{D}_{5/2}$ has a longer radiative lifetime ($A = 12.4 \text{ s}^{-1}$)¹⁷ than the $^2\text{D}_{3/2}$ state. Both Bevan and Husain² and Trainor³ found that the $J = 5/2$ state was removed more rapidly with all collision partners studied than was the $J = 3/2$ state. Therefore, all positive contributions via either radiative transitions or collisional cascading to the $^2\text{D}_{3/2}$ population should take place on a time scale that is short in relation to the exponentially decaying portion of the data on which the removal rates are based.

Our technique for determining decay rates of the $\text{Bi}(^2\text{D}_{3/2})$ state is straightforward. Following the photolysis pulse, we observe an emission signal that rises from some instantaneous value with a time constant on the order of $(0.1\text{--}30) \times 10^5 \text{ s}^{-1}$ (depending on conditions), followed by a slower decay. Such traces can be fit well by a rising plus a falling exponential. Figure 2 provides an example of two representative time histories and their associated

(15) Donovan, R. J.; Husain, D.; Kirsch, L. J. *Trans. Faraday Soc.* **1970**, *66*, 2551.

(16) Moore, C. E., Ed. *Atomic Energy Levels. Natl. Bur. Stand. (U.S.) Circ.* **1958**, No. 467.

(17) Garstang, J. *Res. Natl. Bur. Stand., Sect. A* **1964**, *68*, 61.

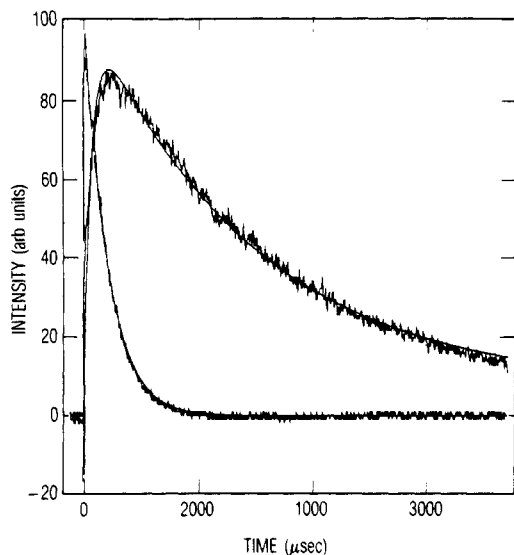


Figure 2. Representative Bi($^2D_{3/2}$) emission traces and associated double-exponential fits. The slower decay was taken with [TMB] = 3.1×10^{12} cm $^{-3}$ in 40 Torr of Ar at 295 K. The more rapidly decaying trace was taken with [H $_2$] = 1.0×10^{18} , [TMB] = 3.1×10^{12} cm $^{-3}$, and balance Ar to 40 Torr. The experimental data are the average of 30 shots. The markedly faster rise time of the trace taken in the presence of H $_2$ is presumably due to cascading into the state via collisions with the quencher.

TABLE I: Rate Coefficients at 295 K for Bi($^2D_{3/2}$) + Q \rightarrow Products

| quencher | k , cm 3 /(molecule-s) | | |
|----------|----------------------------------|------------------------------|-----------------------------|
| | this work | ref 3 | ref 2 |
| Ar | $<2 \times 10^{-17}$ | $<1 \times 10^{-16}$ | |
| CO $_2$ | $<8 \times 10^{-17}$ | $<1 \times 10^{-15}$ | $<4 \times 10^{-15}$ |
| SF $_6$ | $<9 \times 10^{-17}$ | $<6 \times 10^{-16}$ | |
| H $_2$ | $4.1 (0.2) \times 10^{-15}$ | $7.2 (0.3) \times 10^{-15}$ | $7.9 (0.8) \times 10^{-14}$ |
| D $_2$ | $<1.4 (0.1) \times 10^{-16}$ | $<2.5 (1.6) \times 10^{-16}$ | $1.1 (0.3) \times 10^{-14}$ |
| HF | $2.3 (0.2) \times 10^{-14}$ | | |
| DF | $<5.8 (0.5) \times 10^{-16}$ | | |
| TMB | $7.7 (1.4) \times 10^{-11}$ | $1.2 (0.1) \times 10^{-10}$ | |
| CH $_3$ | $\geq 2.6 (0.6) \times 10^{-10}$ | | |

fits for Bi($^2D_{3/2}$) with and without H $_2$ at a total pressure of 40 Torr in Ar. The rate of decay we measure is the sum of the rates of diffusion, spontaneous emission, and removal by the buffer gas, TMB, various photolysis products, and the collision partner of interest. By maintaining cell pressure, TMB partial pressure, and photolysis fluence constant while varying the partial pressure of a particular collision partner, one can determine the dependence upon that species. We obtain removal rate coefficients by plotting the decay rates thus obtained as a function of the number density of the collision partner for a particular set of runs. Figure 3 presents results for quenching by CO $_2$, H $_2$, and HF.

Table I presents absolute rate coefficients for the removal of Bi($^2D_{3/2}$) at 295 K by Ar, CO $_2$, SF $_6$, H $_2$, D $_2$, HF, DF, and TMB. Also given is a lower limit for removal by CH $_3$. The error quoted is at least 2σ based on the linear least-squares fits of the data. Where appropriate, the results of Bevan and Husain 2 and of Trainor 3 are also provided. Where comparisons are possible, our agreement with Trainor is, in most cases, reasonably good. Although our results for H $_2$ and D $_2$ differ from those of Trainor by about a factor of 2, the ratio of the coefficients, k_{H_2}/k_{D_2} , in both instances is in very good agreement (29.3 vs 28.8 for Trainor). Trainor has already discussed the discrepancy between his data and that of Bevan and Husain. We would only add that, like Trainor, we have worked at a significantly lower partial pressure of TMB (0.1 vs 3 mTorr for Bevan and Husain). As a result, because TMB and its CH $_3$ photofragments are efficient quenchers, our measurements are made against a slower background rate, affording us greater sensitivity to slow processes.

The Bi($^2D_{3/2}$) state lies 1.4 eV above the 4S ground state. This excess energy may be disposed of radiatively, through inelastic collisions with the bath gas or through chemical reaction where

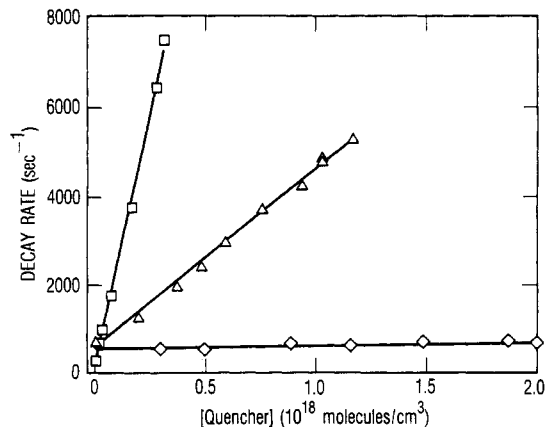


Figure 3. Rate of decay of Bi($^2D_{3/2}$) as a function of number density of the collision partner for CO $_2$ (diamonds), H $_2$ (triangles), and HF (squares) and linear least-squares fits to the data. The variation in the intercepts is due to the differences in the partial pressure of TMB and laser fluence for a given set of runs.

that channel is thermally accessible. Nonreactive quenching may proceed through electronic-to-translational (E \rightarrow T) energy transfer. When the collision partner is polyatomic, energy may also transfer to its internal degrees of freedom (E \rightarrow V, R). The majority of the species studied here display extremely slow removal rate coefficients. Husain and co-workers have made an exhaustive study of the collisional dynamics of the excited electronic state arising from the np^3 ground-state configuration of the group V series. 2,18 Within this series, Bi displays a marked kinetic stability. For collisions with CO $_2$, for example, they report a rate coefficient between 45 and 800 times smaller than those for the $^2D_{3/2}$ state of the other elements of the group. The inefficiency of the removal mechanism in such cases is indicative of a predominately E \rightarrow T process. As will be discussed, in certain instances we observe enhancements to this basic rate which may be adequately explained in terms of near-resonant E \rightarrow V transfer. Finally, the very rapid removal by TMB and CH $_3$ is suggestive of a chemically reactive channel.

The enhanced rate of removal of Bi($^2D_{3/2}$) by H $_2$ relative to D $_2$ and by HF relative to DF is worthy of comment. In both cases the protonated form exhibits kinetics that are notably faster than its deuterated analogue. Ewing 19 has extended the Sharma-Brau theory 20 of V \rightarrow V energy transfer to calculate transition probabilities for near-resonant E \rightarrow V transfer in the relaxation of the excited spin-orbit states of Te and Pb by H $_2$ and D $_2$, respectively. In this treatment energy transfer is accomplished via a long-range attractive potential. For homonuclear diatomics, the coupling is described by a multipole expansion in which the first nonvanishing term is the quadrupole-quadrupole interaction of the initial and final states. In order for us to consider an E \rightarrow V channel, it is necessary to invoke multiple-quantum transitions in the molecular collision partner ($\Delta v = 3$ for H $_2$, $\Delta v = 4$ for D $_2$). Direct application of Ewing's model to Bi($^2D_{3/2}$) predicts a relative mean velocity and J state averaged rate coefficient of 2.4×10^{-14} cm 3 /s for H $_2$ and 2.5×10^{-15} cm 3 /s for D $_2$. These results are a factor of 6 and 20 too large, respectively, compared with our experimentally obtained results for H $_2$ and D $_2$. Table II provides the parameters that we have used in the calculation and their appropriate references.

It is possible to simplify Ewing's formalism to obtain an estimate of the degree to which long-range interactions account for the

- (18) Bevan, M. J.; Husain, D. *J. Photochem.* **1974**, *4*, 51.
- (19) Ewing, J. J. *Chem. Phys. Lett.* **1974**, *29*, 50.
- (20) Sharma, R. D.; Brau, C. A. *J. Chem. Phys.* **1969**, *50*, 924.
- (21) Hertzberg, G. *Spectra of Diatomic Molecules*; Van-Nostrand Reinhold: New York, 1950; Chapter 3.
- (22) Herbelin, J. M.; Emanuel, G. *J. Chem. Phys.* **1974**, *60*, 689.
- (23) Poll, J. D.; Wolniewicz, L. *J. Chem. Phys.* **1978**, *68*, 3053.
- (24) Hirschfelder, J. O.; Curtis, C. F.; Bird, R. B. *Molecular Theory of Gases and Liquids*; Wiley: New York, 1954; p 1110.
- (25) Fischer, C. F. *At. Data* **1972**, *4*, 301.

TABLE II: Parameters Used To Evaluate Long-Range Interaction Probability for Near-Resonant E → V Transfer

| | Bi(² D _{3/2}) | +H ₂ | +D ₂ | +HF | +DF |
|---|-------------------------------------|-------------------------|-------------------------|--------------------------------|---------------------------------|
| transition (<i>v</i> , <i>J</i>) | | 0,2 → 3,0 | 0,0 → 4,2 | 0 → 3 | 0 → 4 |
| Δ <i>E</i> , ^a cm ⁻¹ | | -27.3 | -39.9 | -82.6 | -341 |
| <i>A</i> , ^{b,c} s ⁻¹ | 0.21 (<i>A</i> _Q) | | | 1.17 (<i>A</i> _D) | 0.007 (<i>A</i> _D) |
| <i>Q</i> _{<i>J</i>,<i>J'</i>} , ^{2,d} erg·cm ⁵ | 4.7 × 10 ⁻⁵¹ | 5.6 × 10 ⁻⁵⁸ | 6.8 × 10 ⁻⁵⁹ | | |
| <i>Q</i> _{av,^{2,d} erg·cm⁵} | | 2.9 × 10 ⁻⁵⁸ | 1.0 × 10 ⁻⁵⁹ | | |
| radius, ^{e,f} Å | 1.74 | 1.48 | 1.48 | | |
| σ _c , Å | | 3.22 | 3.22 | | |

^a Reference 21. ^b Reference 17. ^c Reference 22. ^d Reference 23. ^e Reference 24. ^f Reference 25.

quenching mechanism. At the same time, by examination of the isotopic coefficient ratio, k_{H_2}/k_{D_2} , much of the uncertainty in the model (principally σ_c , the collision radius at which the model is evaluated) can be reduced in importance.²⁶ The dominant feature in such a model is the magnitude of the quadrupole moments of the collision partners. By taking the average of the squares of the off-diagonal quadrupole matrix elements, $\Delta J = 0, \pm 2, 0 \leftarrow/\rightarrow 0$, weighted over 99% of the rotational population for H₂ ($\Delta v = 3, J = 0-3$) and D₂ ($\Delta v = 4, J = 0-5$), we obtain a *J*-averaged transition moment and thereby avoid the somewhat arbitrary assignment of a particular rotational level of the collision partner.

$$Q_{av}^2 = \left(\sum_{J,J'} Q_{J,J'}^2 N_J / N_T \right) / n \quad (5)$$

where $Q_{J,J'}$ is the quadrupole matrix element for a particular *J* and ΔJ , N_J/N_T is the relative population in a given *J*, and *n* is the number of transitions over which the sum is taken. The transition probability is proportional to the quotient of the square of the quadrupole moment and the square of the average velocity of the collision pair:

$$P \propto Q^2 / v^2 \quad (6)$$

The rate coefficient, in turn, is the product of the probability and the average velocity of the collision pair:

$$k = Pv \propto Q^2 / v \quad (7)$$

The isotopic ratio, then, is

$$k_{H_2}/k_{D_2} = Q_{H_2}^2 v_{D_2} / Q_{D_2}^2 v_{H_2} \quad (8)$$

Note that we have not explicitly considered the energy defect of the collision. By averaging Q^2 over available *J* levels, we have implicitly included near-resonant collisions. Performing this calculation, we obtain $k_{H_2}/k_{D_2} = 19.9$. While this result is smaller than the observed ratio of 29.3, it is in close enough agreement to suggest that the mechanism is a plausible one.

Pritt and Coombe²⁷ have suggested a long-range E → V transfer mechanism for I* quenching by HF/HCl where the interaction potential may be described in terms of dipole-quadrupole coupling. Their results are normalized by a factor proportional to the product of the squares of dipole transition moment of the molecule and quadrupole transition moment of the atom

$$k_{nor} = k_{E-V} (A_D \lambda_D^3 A_Q \lambda_Q^5)^{-1} \quad (9)$$

where A_D and λ_D are the spontaneous emission coefficient and wavelength of the molecular dipole vibrational transition of interest and A_Q and λ_Q are the corresponding atomic quadrupole terms. Rotational energy is not considered. Carrying out this procedure for Bi(²D_{3/2}) + HF/DF gives

$$k_{HF,nor} = 2.6 \times 10^{-13} \text{ cm}^3 / (\text{molecule} \cdot \text{s}^3 \cdot \mu\text{m}^8); \quad \Delta E = -83 \text{ cm}^{-1}$$

$$k_{DF,nor} = 8.5 \times 10^{-13} \text{ cm}^3 / (\text{molecule} \cdot \text{s}^3 \cdot \mu\text{m}^8); \quad \Delta E = -341 \text{ cm}^{-1}$$

Pritt and Coombe compared their normalized values to the results of previous work in which E → V transfer has been established as the dominant relaxation channel for Br* + HX⁵ by means of

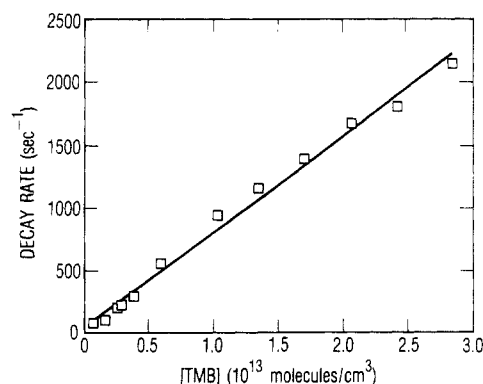


Figure 4. The decay rate of Bi(²D_{3/2}) as a function of TMB density. The rates were deduced from the *y* intercepts of plots of the rate of decay of the ²D_{3/2} state vs laser fluence at a fixed concentration of TMB. This is a true Stern-Volmer plot; the *y* intercept is the inverse radiative lifetime of Bi(²D_{3/2}).

a Lambert-Salter plot of $\log k_{nor}$ vs $-\Delta E$. Our results for $k_{HF,nor}$ is within 25% of the fitted value of the data they present. The value obtained for $k_{DF,nor}$ is about a factor of 5 too large, given the exothermicity of the transfer. Considering the simplicity of the model, we feel that these results are indicative of the existence of an E → V relaxation channel.

Trainor³ has quoted a rate coefficient for the removal of ²D_{3/2} by TMB with the caveat that it represents a weighted average of TMB and all photolysis products. We have deduced a rate coefficient for TMB and set a lower limit on the rate coefficient for the CH₃ photofragments.

The rate coefficient for the removal of Bi(²D_{3/2}) by the parent TMB was arrived at in the following manner. A range of photolysis fluences was established for which decay rates demonstrated a sensibly linear dependence (<5 mJ/cm²). A set of runs with constant [TMB] were conducted in which fluences were varied within that range. The decay rate for each of these runs was determined and plotted as a function of photolysis power. The *y* intercept from the linear least-squares fit to this data is the extrapolated rate of removal of the ²D_{3/2} state in the absence of photolysis and therefore in the absence of any photolysis products. This procedure was repeated for a number of partial pressures of TMB. The zero-power intercepts from the resulting plots were, in turn, plotted as a function of their corresponding TMB number density (Figure 4). The slope of a linear least-squares fit to the data is the rate coefficient for removal by TMB; the intercept should correspond to the inverse radiative lifetime of Bi(²D_{3/2}). This is indeed the case; we obtain an intercept of 33.2 s⁻¹ that may be compared to Garstang's calculation¹⁷ for the sum of the Einstein *A* coefficients for electric quadrupole and magnetic dipole radiation of 31.2 s⁻¹.

To derive a lower limit on the rate coefficient for CH₃, we make the assumption that the absorption of one 193-nm photon results in the complete decomposition of the parent molecule



If one uses the bond energies of Price and Trotman-Dickenson,²⁸

(26) French, N. P. D.; Lawley, K. P. *Chem. Phys.* **1976**, *22*, 105.
(27) Pritt, A. T.; Coombe, R. D. *J. Chem. Phys.* **1976**, *65*, 2096.

(28) Price, S. J. W.; Trotman-Dickenson, A. F. *Trans. Faraday Soc.* **1958**, *1630*.

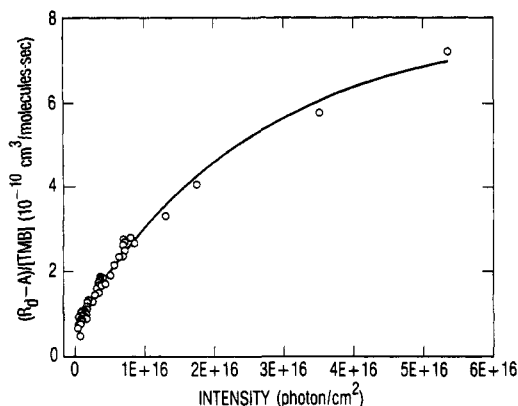


Figure 5. Experimental data corresponding to the case described by eq 17. Each point represents the total collisional decay rate of Bi(²D_{3/2}) for a particular TMB density and photolysis fluence. The fit displayed with the data is a least-squares single exponential in which the base line is one of the parameters to be determined.

the three Bi-CH₃ bonds contain a total of 101.4 kcal/mol or about 35 500 cm⁻¹. The Bi(²D_{3/2}) state lies 11 419 cm⁻¹ above the ⁴S^o ground state. It is therefore energetically possible for a single 193-nm photon (51 813 cm⁻¹) to provide the requisite energy to cleave the three methyl bonds and populate the ²D_{3/2} level. The following argument is valid, however, so long as eq 10 is correct, even if the complete dissociation is a multiple-photon process.

The overall rate of decay of the ²D_{3/2} state may be written as

$$R_d = A + k_1[\text{TMB}] + k_2[\text{CH}_3] \quad (11)$$

where *A* is the Einstein coefficient for spontaneous emission. According to our assumption

$$[\text{TMB}] = [\text{TMB}]_0 - [\text{CH}_3]/3 \quad (12)$$

$$R_d = A + k_1[\text{TMB}]_0 + (k_2 - k_1/3)[\text{CH}_3] \quad (13)$$

The fraction of TMB dissociated is

$$[\text{TMB}]_{\text{dis}}/[\text{TMB}]_0 = 1 - \exp(-\sigma I) \quad (14)$$

where σ is the absorption cross section and *I* is the laser intensity in photons/cm² at $\lambda = 193$ nm. Therefore

$$\text{CH}_3 = 3[\text{TMB}]_0(1 - \exp(-\sigma I)) \quad (15)$$

$$R_d = A + [\text{TMB}]_0\{k_1 + (3k_2 - k_1)(1 - \exp(-\sigma I))\} \quad (16)$$

Finally, we can write

$$(R_d - A)/[\text{TMB}]_0 = 3k_2 - (3k_2 - k_1) \exp(-\sigma I) \quad (17)$$

This is the case for the data presented in Figure 5. The plotted rates are obtained from power-dependence measurements at fluences of up to about 55 mJ/cm². The accompanying fit is of the form

$$y = A_1 \exp(A_2 x) + A_3$$

This fit gives a rate coefficient for ²D_{3/2} removal by CH₃ (*k*₂) of 2.6 × 10⁻¹⁰ cm³/(molecule-s). The coefficient for removal by TMB (*k*₁) is 7.1 × 10⁻¹¹, which is in excellent agreement with the value of 7.7 × 10⁻¹¹ obtained by using the zero-power intercept method. Note that our values for TMB and CH₃ bracket Trainor's value of 1.2 × 10⁻¹⁰ for quenching by TMB and photofragments. A value for the absorption cross section of TMB at 193 nm, $\sigma = 3.9 \times 10^{-17}$ cm², is also arrived at in the fit. Independent measurements of a purified sample of TMB on a ultraviolet spectrometer at 193 nm yielded a value for σ of 3.8 × 10⁻¹⁷ cm². These same absorption measurements gave a value for σ at 211.5 nm of 5.4 × 10⁻¹⁷ cm² within 15% of the literature value of 6.3 × 10⁻¹⁷ cm².¹ The fact that our model yields values for *k*₁ and σ which are in good agreement with independent measurements of those same quantities not only leads us to believe that our value for *k*₂ is a valid lower limit but also suggests that the model itself is a plausible representation of at least one of the processes leading to Bi production following photolysis. If so, *k*₂ may be interpreted as an absolute value.

IV. Summary

The rate coefficients for the spin-orbit relaxation of Bi(²D_{3/2}) by a number of nonreactive collision partners have been measured at 295 K. For Ar, CO₂, and SF₆ the rates are slow, *k* < 1 × 10⁻¹⁶ cm³/(molecule-s). For H₂ and HF, we observe rates that are substantially faster than for their deuterated analogues, D₂ and DF. This isotope effect may be adequately explained in terms of near-resonant, multiquantum E → V transfer via a long-range multipole interaction. We have also determined a rate coefficient for quenching by the photolytic precursor, TMB. We present a simple kinetic model that allows us to place a lower limit on the rate of removal by CH₃ photofragments.

Acknowledgment. We express our gratitude to the Air Force Weapons Laboratory and Capt. Glen Perram for their continuing support of this research. We also extend our thanks to J. F. Bott for his help with the methyl radicals kinetics and J. M. Herbelin for insight into the NF/BiF system. This work was conducted under U.S. Air Force Space Division (AFSD) Contract No. F04701-88-C-0089.

Registry No. TMB, 593-91-9; Bi, 7440-69-9; SF₆, 2551-62-4; H₂, 1333-74-0; D₂, 7782-39-0; HF, 7664-39-3; DF, 14331-26-7; Ar, 7440-37-1; CO₂, 124-38-9; Me[•], 2229-07-4.